International Journal of Thermophysics, Vol. 21, No. 6, 2000

Novel Phase-Transition Behavior in an Aqueous Electrolyte Solution[1]

J. Jacob,[2,3] M. A. Anisimov,[2,4] A. Kumar,[3] V. A. Agayan,[2] and J. V. Sengers[2]

Received May 1, 2000

We have investigated the near-critical behavior of the susceptibility of a ternary liquid mixture of 3-methylpyridine, water, and sodium bromide as a function of the salt concentration. The susceptibility was determined from light-scattering measurements performed at a scattering angle of 90° in the one-phase region near the locus of lower consolute points. A sharp crossover from asymptotic Ising behavior to mean-field behavior has been observed at concentrations ranging from 8 to 16.5 mass% NaBr. The range of asymptotic Ising behavior shrinks with increasing salt concentration and vanishes at a NaBr concentration of about 17 mass%, where complete mean-field-like behavior of the susceptibility is observed. A simultaneous pronounced increase in the background scattering at concentrations above 15 mass%, as well as a dip in the critical locus at 17 mass% NaBr, suggests that this phenomenon can be interpreted as mean-field tricritical behavior associated with the formation of a microheterogeneous phase due to clustering of the molecules and ions. An analogy with tricritical behavior observed in polymer solutions as well as the possibility of a charge-density-wave phase is also discussed. In addition, we, have observed a third soap-like phase on the liquid–liquid interface in several binary and ternary liquid mixtures.

KEY WORDS: aqueous ionic solutions; critical phenomena; crossover; light scattering.

[1] Paper presented at the Fourteenth Symposium on Thermophysical Properties, June 25–30, 2000, Boulder, Colorado, U.S.A.

[2] Institute for Physical Science and Technology and Department of Chemical Engineering, University of Maryland, College Park, Maryland 20742, U.S.A.

[3] Department of Physics, Indian Institute of Science, Bangalore 560 012, India.

[4] To whom correspondence should be addressed. E-mail: anisimov@glue.umd.edu.

0195-928X/00/1100-1321$18.00/0

1. INTRODUCTION

Critical phenomena in complex fluids such as ionic solutions, polymer solutions, micellar solutions, etc., continue to be an active topic of both theoretical and experimental research [1–6]. Asymptotically close to the critical point, fluids, both simple and complex, are expected to belong to the Ising universality class [1, 2]. In complex fluids, however, the interplay between universality caused by long-range fluctuations of the order parameter and a competing mesoscopic supra- or macromolecular structure may affect the approach to universal critical behavior. Hence, even within the Ising universality class, complex fluids may exhibit different crossover behavior upon approaching the critical point.

In polymer solutions the crossover from mean-field-like behavior to asymptotic Ising behavior occurs closer to the critical point as the molecular weight of the polymer increases [7]. This crossover can be explained in terms of a competition between the correlation length ξ of the critical fluctuations and the radius of gyration R_g of the polymer molecules [7]. Polymer solutions exhibit a tricritical *theta* point in the limit of infinite molecular weight ($R_g \to \infty$) of the polymer [8]. The critical behavior near a tricritical point in three dimensions is a mean-field one with small logarithmic corrections [9]. Hence, the crossover observed in polymer solutions is, in fact, from the asymptotic Ising regime to the mean-field tricritical regime.

In ionic solutions the phase separation can be driven by either Coulombic interactions (low-dielectric constant solvents) or solvophobic interactions (high-dielectric constant solvents). In both cases, asymptotically close to the critical point, Ising-like behavior is expected due to a screening effect in the first case and due to short-range forces in the second case [2]. Experiments on ionic solutions have revealed either Ising, mean-field, or a crossover behavior between these two regimes [5]. A crossover from Ising behavior to mean-field behavior has been observed in several low-dielectric constant "Coulombic" ionic solutions [10], although the correlation between the value of the dielectric constant and the crossover behavior has not been confirmed by other investigators.

To investigate the nature of criticality in aqueous ionic solutions, we have performed a series of light-scattering measurements in the ternary liquid mixture 3-methylpyridine (3MP) + water (H_2O) + sodium bromide (NaBr) [11]. The phase separation in this system is driven by solvophobic interactions in which hydrogen bonds between 3MP and H_2O play an important role. Light-scattering measurements reveal that the effective critical exponent γ_{eff} for the osmotic susceptibility χ exhibits a crossover from the three-dimensional Ising asymptotic value ($\gamma = 1.24$) close to the critical temperature (T_c) to the mean-field value ($\gamma = 1.00$); this crossover behavior

becomes more and more pronounced as the concentration of NaBr increases [11]. In this paper we show that for a sample with a concentration of 17 mass% NaBr, complete mean-field behavior has been observed in the entire temperature range investigated. Moreover, a simultaneous pronounced increase in the background scattering appearing at the higher salt concentrations suggests that this phenomenon is to be interpreted as mean-field tricritical behavior associated with the appearance of a microheterogeneous phase due to clustering of ions and molecules.

2. EXPERIMENT

3-Methylpyridine and water are miscible in all proportions at atmospheric pressure over the entire liquid-state temperature range (from freezing to boiling points of the liquids). However, a closed-loop immiscibility region with loop size $\Delta T = T_U - T_L$ (T_U and T_L being the upper and lower critical solution temperature, respectively) appears when the mixture with 30 mass% 3MP is subjected to a pressure of approximately 130 MPa [12]. A similar effect can be realized by the addition of ~ 0.1 mass% of sodium chloride or ~ 0.4 mass% of NaBr to the mixture (Fig. 1). With further addition of electrolyte, the gap ΔT increases. At the "double" critical point, at which the lower and upper critical points coincide, the asymptotic critical exponents are doubled [13]. Hence, the effective values of the critical exponents will appear to be larger than their actual asymptotic values if ΔT is small. However, it has been demonstrated in earlier investigations of the system $3MP + H_2O + D_2O$ [13] that the critical exponents do not exhibit any noticeable increase beyond their Ising values when the loop size (ΔT) is large (in practice, for $\Delta T \gtrsim 70$ to 80°C). Hence, for large enough values of ΔT, the presence of the upper critical point can be neglected for measurements near the lower critical point. In the case of $3MP + H_2O + NaBr$, it can be noted from Fig. 1 that even at a concentration of 5 mass% NaBr, the size of the closed loop is larger than 100°C. We also note that the lower critical temperatures are easily accessible experimentally over a wide range of electrolyte concentrations, if NaBr is used in comparison to other electrolytes such as sodium chloride, potassium bromide, sodium iodide, etc. The critical temperatures were also found to be stable in this system; the drift in T_L was less than 0.01°C over a period of 2 years.

Samples for our light-scattering measurements were prepared with 3MP (Aldrich; 99% pure), water (triple distilled in an all-quartz distiller), and analytical-grade NaBr (99% pure). The critical composition of 3MP, $x_{MP} = (x_{MP})_c$ (x_{MP} being the mole fraction of 3MP in the ternary mixture), at each concentration of NaBr was accurately determined by choosing the concentration of the sample at which equal-volume phase separation

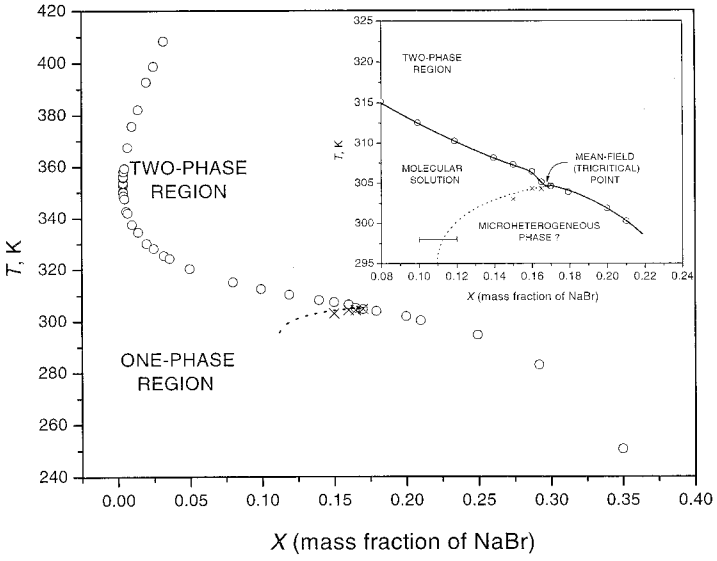

Fig. 1. Phase diagram of the 3-methylpyridine + water + NaBr system. The inset shows an expanded view of the range of NaBr concentrations where light-scattering measurements have been performed. The solid curve indicates the critical phase-separation line and the dashed curve bounds the temperature and salt concentrations where a microheterogeneous phase exists. The crosses indicate the temperatures corresponding to $\tau = \tau_0$ according to Eq. (4) where clustering appears. The horizontal bar indicates the concentration range at $T = 298$ K, where clustering appears according to SAXS measurements.

occurs at the phase-separation temperature. This procedure was repeated at each concentration of NaBr, since x_{MP} varies with the NaBr concentration. The lower critical temperatures were measured in a well-stirred liquid-paraffin thermostat with temperature stability better than ± 5 mK. The critical temperature was determined by visual observation of the onset of phase separation and the eventual formation of an interface when the temperature is changed in steps of 2 to 3 mK. We have also ascertained the value of T_L before and after measuring the scattered-light intensity by monitoring the vanishing of the transmitted laser beam. For samples with $X > 0.16$ (X denotes the overall mass fraction of NaBr in the mixture), critical opalescence could be observed only in a narrow range of temperatures close to the critical point, whereas, for samples with $X < 0.16$, critical opalescence starts farther away from T_L.

The samples (volume, ~ 5 cm^3) were initially prepared in cylindrical pyrex glass cells and then transferred into the optical cells (volume,

~ 0.3 cm^3) by means of airtight (Hamilton) syringes fitted with Millipore filters (pore size, 0.2 μm). These cells were flame-sealed after the samples had been frozen in liquid nitrogen. A brass-block thermostat with a temperature stability better than ± 1 mK was used in the light-scattering measurements. The laser beam ($\lambda = 632.8$ nm) from a He–Ne laser (5 mW) was focused at the center of the sample. The intensity of scattered light I was measured at 90° by photon counting. The transmitted and incident beam intensities were measured with photodiodes. The light-scattering intensity data were normalized with respect to the incident-light intensity to account for fluctuations in the incident light. Corrections due to increased turbidity near the critical point have also been incorporated [14]. Figure 2 shows the total scattered intensity I as a function of $\tau = (T_L - T)/T$ for different X.

A crucial difference in the data-acquisition procedure for samples with $X \leqslant 0.16$ and $X > 0.16$ should be mentioned. Samples with $X \leqslant 0.16$ were well stirred for about 15 to 20 min in an ultrasonic agitator after preparation and also before starting each light-scattering run. However, in the case of samples with $X > 16$ mass% NaBr, a different procedure had to be adopted for measuring the scattered intensity. The samples were agitated in the ultrasonic agitator and then mounted in the thermostat at the temperature

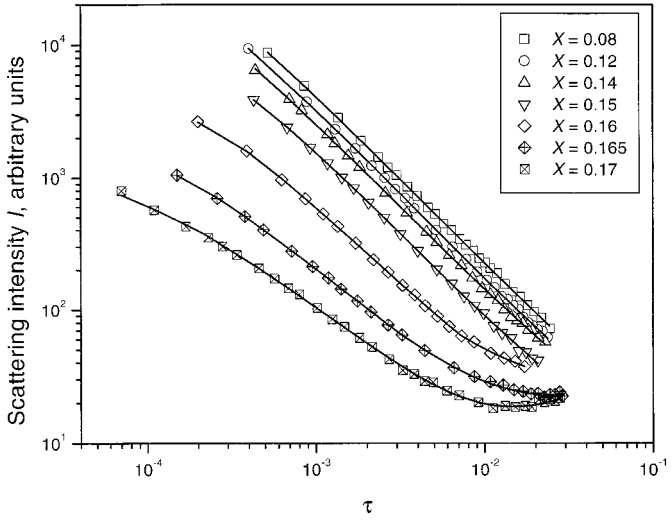

Fig. 2. Light-scattering intensity I as a function of τ for samples with seven mass fractions of NaBr. The symbols denote the experimental data, and the curves represent values calculated from the crossover model with a correction for enhanced background scattering due to cluster formation for $X \geqslant 0.16$.

where the light-scattering measurements would begin. Moreover, the samples were left undisturbed for about 24 h before we actually started the measurements. Reproducible data from different experiments on the same sample were obtained only if this protocol was followed. Thermal equilibrium was indicated by the invariance of the scattered and transmitted intensities with time. The typical equilibration time for a temperature step of 0.1 K (for the undisturbed sample) was ~ 20 to 25 min, which we found to be approximately the same for all concentrations. However, for samples with $X \geqslant 0.18$, it was not possible to obtain reproducible data even by following this procedure and the light-scattering intensity showed deviations of up to 5% from a simple dependence on the reduced temperature τ. We think that this may be due to unusually long equilibration times for these samples with high salt concentrations. Hence, we have not attempted to analyze comprehensively the data for samples with $X \geqslant 0.18$.

3. RESULTS AND DISCUSSION

The intensity of light scattered by critical fluctuations I_c in fluids can be represented by

$$I_c = \frac{C\chi}{1 + q^2\xi^2} \tag{1}$$

where χ is the susceptibility, ξ is the correlation length, C is an experimental constant, and q is the wave number, which is related to the scattering angle θ ($\theta = 90^\circ$ in our case) as $q = 4\pi n/\lambda_0 \sin(\theta/2)$, where $\lambda_0 = 632.8$ nm, the wavelength of the incident light (in vacuum), and n is the refractive index. The dependence of the light-scattering intensity on the wave number q given by Eq. (1) is not exact [15] for large values of $q\xi$ but any deviations are negligible for the wave numbers probed in our experiment. The intensity of light-scattering due to the critical fluctuations in the limit of zero wave number is proportional to the critical susceptibility χ, which diverges at the critical point. In a binary liquid solution, the susceptibility is proportional to the osmotic compressibility $(\partial x_2/\partial \mu_{2-1})_{P,T}$, where x_2 is the concentration (mole fraction) of the solute and $\mu_{2-1} = \mu_2 - \mu_1$, the difference between solute and solvent chemical potentials conjugate to x_2.

In a ternary liquid solution, the critical susceptibility is proportional to a generalized osmotic compressibility defined as $\chi = (\partial x_2/\partial \mu_{2-1})_{P,T,\mu_{3-1}}$, with $\mu_{3-1} = \mu_3 - \mu_1$ being the chemical potential difference of the third component and the solvent conjugate to x_3 (since $d\mu_1 + x_2\, d\mu_{2-1} + x_3\, d\mu_{3-1} = 0$ at constant P and T). The generalized susceptibility and the

correlation length exhibit the asymptotic singular behavior $\chi = \Gamma_0 \tau^{-\gamma}$ and $\xi = \xi_0 \tau^{-\nu}$, respectively, where Γ_0 and ξ_0 are system-dependent critical amplitudes, and where the critical exponents $\gamma = 1.24$ and $\nu = 0.63$ are universal, provided that the chemical potential difference $\mu_{3-1} = \mu_3 - \mu_1$ is constant. However, the light-scattering measurements are performed at a constant overall concentration ($x_3 = \tilde{X}$, the overall mole fraction of NaBr) and, as a consequence, the experimentally observed asymptotic critical-exponent values are affected by Fisher renormalization [16]. As a consequence, the susceptibility exponent changes its asymptotic value from γ to $\gamma/(1-\alpha)$ with $\alpha = 0.11$, the critical exponent of the so-called weakly divergent susceptibility [17]. In our data analysis, we have accounted for this Fisher renormalization by expressing the experimental temperature scale $\tau(\tilde{X})$ through the theoretical temperature scale $\tau = \tau(\mu_{3-1})$ [18]:

$$\frac{\tau(\tilde{X})}{\tau_2} \cong \left(\frac{\tau(\mu_{3-1})}{\tau_2}\right)^{1-\alpha} \left[1 + \left(\frac{\tau(\mu_{3-1})}{\tau_2}\right)^{\alpha}\right] \tag{2}$$

where the characteristic temperature τ_2 is defined by

$$\tau_2 = \left[A_0 \tilde{X}(1-\tilde{X}) \left(\frac{1}{T_c}\frac{dT_c}{d\tilde{X}}\right)^2 \right]^{1/\alpha} \tag{3}$$

Here A_0 is the critical amplitude of the weakly divergent ($\sim \tau^{-\alpha}$) susceptibility, which is related to the amplitude ξ_0 of the power law for the correlation length by a universal two-scale-factor relation [11]. The extent and observability of Fisher renormalization depend on the parameter τ_2, and, hence, on the concentration $\tilde{X}$ and the slope of the line of critical temperatures versus $\tilde{X}$, $(dT_c/d\tilde{X})$. In the mean-field regime where $\alpha = 0$, Fisher renormalization disappears.

In analyzing data in terms of Eq. (1), χ and ξ have been represented by equations from a crossover theory, which recovers Ising asymptotic behavior with Wegner corrections close to the critical point and mean-field behavior far away from the critical point [19]. For samples with $X \geqslant 0.16$, the total intensity includes a contribution from background scattering also. The intensity of the background scattering I_0 was calculated as the difference between the total intensity I and the intensity I_c from the critical fluctuations. As an alternative approach, the data, including those far away from the critical point, were fitted with the expression $I = I_c + I_0$, where I_0 was represented by

$$I_0 = m_1(\tau - \tau_0) + m_2(\tau - \tau_0)^2 \tag{4}$$

and τ_0, m_1, and m_2 are adjustable parameters (Table I). Physically, Eq. (4), which is similar to the virial-like expression expected near the critical micellar concentration [20], corresponds to the assumption that the formation of "clusters" emerges at a certain $\tau = \tau_0(X)$. The crossover behavior of χ and ξ obtained with these two alternative treatments of the background scattering appeared to be essentially the same. From Figs. 2 and 3 it can be seen that I_0 is negligible at $X \leqslant 0.15$, but it becomes increasingly prominent with an increase in X. Small-angle X-ray scattering (SAXS) studies in these solutions have provided evidence for cluster formation in samples with $X \geqslant 0.12$ [21]. A systematic increase in cluster size with concentration was shown in the range $0.12 \leqslant X \leqslant 0.17$. This clustering was explained as due to the formation of 3MP-rich clusters resulting from a preferential solvation of Na^+ and Br^- ions by water molecules [21]. Evidence of clustering induced by potassium chloride in a somewhat similar solution of 1-propanol and water has also been provided by small-angle neutron-scattering measurements [22]. Therefore, the temperature $\tau = \tau_0(X)$ in Eq. (4) can be interpreted as the temperature of cluster formation and can be determined experimentally. Figure 3 shows the relative excess scattering intensity, defined as $I_0/(I_c + I_0)$, as a function of the distance to the critical temperature. It can be seen that the emergence of the "background" scattering coincides with the critical temperature somewhere above $X = 0.165$ and slightly below $X = 0.17$.

The crossover to mean-field behavior is generally controlled by two physical parameters, namely, a rescaled coupling constant $\bar{u}$ which reflects the range of molecular forces and a so-called "cutoff" [4, 7, 19]. In simple fluids the "cutoff" is related to the molecular size and the trend to mean-field critical behavior is controlled by the coupling constant only. In complex fluids the "cutoff" is associated with a characteristic supramolecular or macromolecular length $\xi_D = v_0^{1/3} \Lambda^{-1}$ representing a crossover length scale [1], with v_0 being an average molecular volume ($v_0^{1/3} \cong 3.5$ Å for our samples [11]), while Λ is a dimensionless characteristic cutoff wave number. If ξ_D is large enough, it competes with the correlation length ξ of the critical fluctuations and controls a crossover to mean-field tricritical (or, more generally, multicritical) behavior. When both ξ and ξ_D diverge, one will recover a mean-field tricritical point.

It is important to emphasize the physical difference between approaching mean-field behavior due to the long-range nature of the molecular forces (small $\bar{u}$, while ξ_0/ξ_D is not low) and that due to a low ratio ξ_0/ξ_D (i.e., the ratio ξ_D/ξ_0 is high, while $\bar{u}$ is not necessarily small). The former case is the conventional crossover to mean-field critical behavior. Complete crossover of such a kind has been observed in the three-dimensional Ising model with a variety of interaction ranges [23, 24]. The latter case of large and

Table I. Parameters for Description of Crossover Behavior of the Light-Scattering Intensity in 3-Methylpyridine + Water + NaBr Solutions

Critical parameters		Crossover parameters			Background light-scattering parameters		
X^a	T_c (K)	$t_\times$	ξ_0 (Å)	ξ_D (Å)	τ_0	m_1	m_2
0.16	306.435 ± 0.004	3×10^{-3}	2.7	70.3	2.1	0.14	0.006
0.165	305.131 ± 0.004	3×10^{-4}	2.4	230	0.96	0.17	0.016
0.17	304.628 ± 0.004	$< 3 \times 10^{-5}$	—	$> 3 \times 10^3$	−0.15	0.04	0.061
0.18	303.888 ± 0.004		not defined		−0.22	0.25	0.19

[a] X denotes the overall mass fraction of NaBr in the mixture.

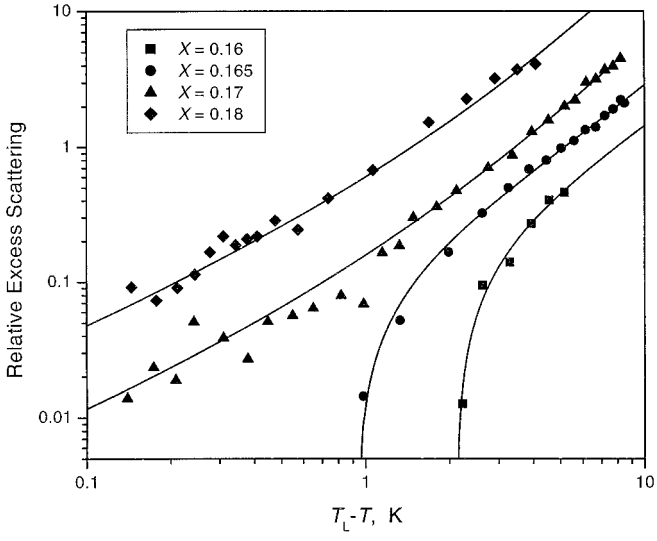

Fig. 3. The relative excess scattering $I_0/(I_0+I_c)$ as a function of the distance to the critical point $(T_L - T)$ for samples with $X \geqslant 0.16$. The solid and dashed curves represent fits to the data in terms of Eq. (4).

eventually diverging ξ_D corresponds to approaching a special kind of mean-field behavior, namely, tricritical mean-field behavior. A typical and conceptually well-understood example is the crossover to theta-point tricriticality in polymer solutions [25].

One may obtain an empirical crossover temperature $\tau_\times$ as the value of τ where the effective susceptibility exponent, defined as $\gamma_{\text{eff}} = -\tau d \ln \chi / d\tau$, and recovered after accounting for Fisher renormalization, exhibits an inflection point as a function of τ [7, 11]. We have found crossover behavior from Ising critical behavior asymptotically close to the critical temperature to mean-field critical behavior farther away from the critical temperature at all salt concentrations up to and including $X = 0.165$. However, the range of Ising critical behavior shrinks with increasing salt concentration. In Fig. 4 we compare the deviations from Ising behavior at the higher salt concentrations with those at the lowest salt concentration $X = 0.08$. At $X = 0.08$ all experimental data are in the crossover regime; at $X = 0.16$ a substantial fraction of the experimental data exhibits mean-field critical behavior; at $X = 0.165$ the experimental data follow the mean-field curve except for the two data points closest to T_c, and at $X = 0.17$ the parameter Λ becomes insignificantly small and the crossover temperature becomes undetectable (Table I). Thus, within our experimental resolution, complete mean-field critical behavior is observed at $X = 0.17$.

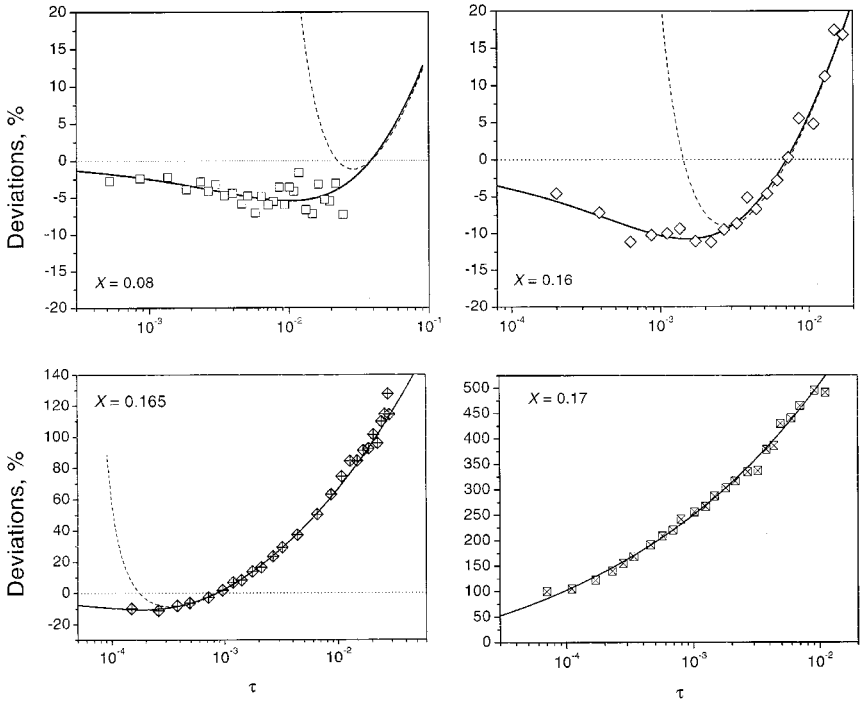

Fig. 4. Deviations of the scattering intensity from asymptotic Ising critical behavior as a function of $\tau = (T_c - T)/T$ for four salt concentrations. The symbols designate experimental data. The dashed curves represent mean-field behavior and the solid curves represent the actual behavior as calculated from the crossover model with a correction for enhanced background scattering for $X \geqslant 0.16$. The solid curve for $X = 0.17$ corresponds to a crossover fit with the insignificant crossover temperature $\tau_\times = 3 \times 10^{-6}$ and coincides with the mean-field (dashed) curve.

In Fig. 5 we show the effective susceptibility exponent γ_{eff} as a function of the reduced temperature τ. It is evident from this figure that the crossover from Ising-like to mean-field behavior becomes more pronounced at higher NaBr concentrations. For the samples with $X = 0.16$, and 0.165, the crossover is practically completed within the critical domain. At $X = 0.17$ we did not find any trend to Ising behavior near the critical point and the observed susceptibility retained mean-field behavior upon the approach to T_c. In addition, the crossover parameter Λ becomes insignificantly small and the crossover temperature $\tau_\times$ becomes undetectably low.

In Fig. 6 we show the crossover temperature $\tau_\times$ and the crossover length scale ξ_D as a function of the salt concentration. As follows from the theory of crossover from Ising critical behavior to mean-field tricritical

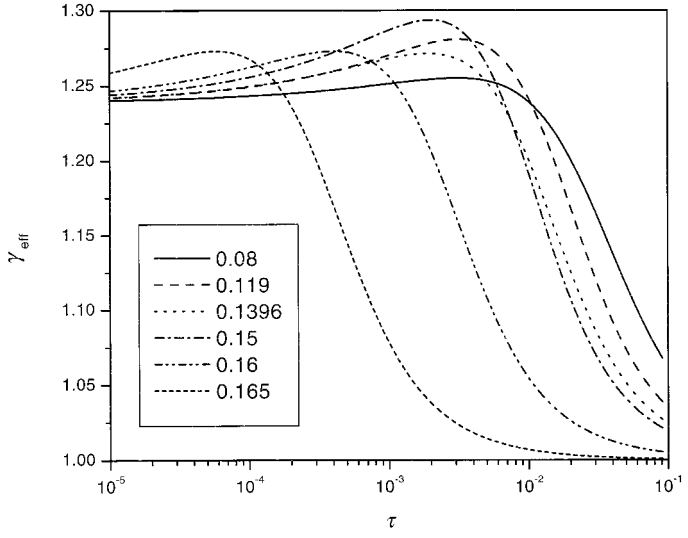

Fig. 5. Effective susceptibility exponent $\gamma_{\text{eff}} = -\tau d \ln \chi / d\tau$ for seven salt concentrations calculated from the crossover model after accounting for Fisher renormalization.

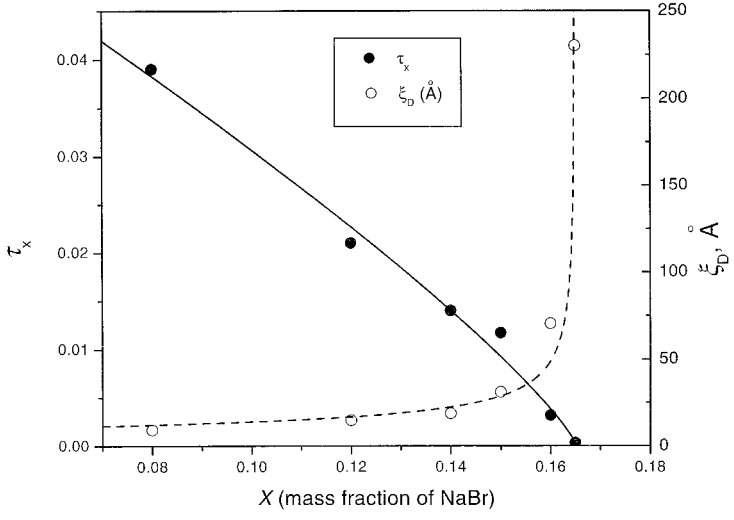

Fig. 6. The crossover temperature $\tau_\times$ and the crossover length scale ξ_D as a function of the salt concentration. The solid curve represents an empirical power law, $\tau_\times \propto (X_0 - X)^{0.8}$, with $X_0 = 0.1652$. The dashed curve represents a power law, $\xi_D \propto (X_0 - X)^{-1/2}$.

behavior [4], at $\tau = \tau_\times$ the correlation length ξ of the critical fluctuations is equal to the competing correlation length ξ_D associated with an additional order parameter. It is seen that the crossover temperature $\tau_\times$ vanishes and the crossover length ξ_D diverges at a salt concentration between 16.5 and 17%. Thus both ξ and ξ_D diverge at this point, giving strong evidence for tricriticality.

The most interesting and intriguing question to be discussed is the physical nature of the discovered mean-field-like multicritical point. There are several possible scenarios of multicritical behavior in a ternary mixture, each of them requiring further investigation. Here we just briefly discuss some phenomenological consequences of these scenarios.

(a) *A fluid-mixture vapor–liquid–liquid tricritical point.* In a ternary fluid mixture there might exist a tricritical point, defined as a point at which two lines of critical end points merge and three near-critical fluid phases become identical [26]. Such a scenario does not look realistic for a ternary liquid solution at atmospheric pressure, as one of the fluid phases along the line of critical end points should originate from the near-critical vapor phase.

(b) *A tricritical point caused by a coupling between two order parameters belonging to different universality classes.* If we assume that an additional (vector-like) order parameter emerges in the system, there might be a coupling between the scalar order parameter (concentration) associated with the liquid–liquid phase separation and this vector-like order parameter associated with some kind of structural ordering in the one-phase region. A projection of this hypothetical phase diagram on the $T-\mu_{3-1}$ plane is shown in Fig. 7. In this figure the λ-line (dotted line) is a line of second-order phase transitions between two macroscopically homogeneous, but structurally different, phases. A coupling between the formation of a microheterogeneous (e.g., micellar-like or microemulsion sponge-like) phase and liquid–liquid phase separation can lead to tricritical behavior [20]. At the tricritical point the λ-line merges with two wings, each of them being the critical liquid–liquid phase separation line. Each wing belongs to an opposite sign of the "ordering field" h, a linear combination of μ_{3-1}, μ_{2-1}, and T. At negative h, two molecular solutions coexist in the two-phase region. At positive h, two microheterogeneous solutions coexist. Along the λ-line, the "ordering field" h is zero with the tricritical point separating the second-order and first-order transitions (shown in Fig. 7 as the dashed line). Along

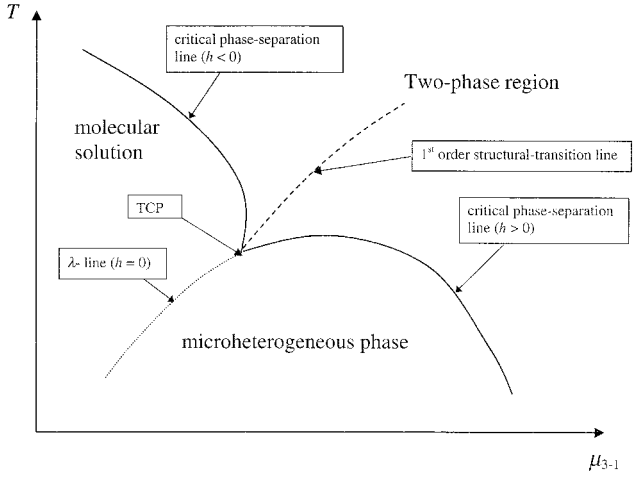

Fig. 7. General schematic phase diagram representing a ternary system with a tricritical point (TCP) emerging as a result of coupling between two order parameters.

the first-order transition line, the molecular solution and microheterogeneous solutions are in liquid–liquid coexistence, and change in the fluid structure is accompanied by phase separation. Such a diagram can be compared with the actual phase diagram of the ternary mixture $3MP + H_2O + NaBr$ shown in Fig. 1.

(c) *The λ-line shown in Fig. 7 corresponds to a transition between a molecular-solution phase and a microheterogeneous phase characterized by an equilibrium mesoscopic wave number, and the tricritical point becomes a so-called Lifshitz point* [27]. In this particular case, the right wing of the critical phase-separation line shown in Fig. 7 will become a first-order liquid–liquid phase separation between the molecular solution and a microheterogeneous phase. The liquid–liquid coexistence between two microheterogeneous phases (the dashed curve in Fig. 7) will not appear. Physically, it means that the microheterogeneous structure becomes unstable with the onset of phase separation. The first-order phase separation will become continuous at a Lifshitz point. Such a scenario seems to be quite plausible. The possibility of a multicritical Lifshitz point in which two fluid phases in an electrolyte solution coexist with a microheterogeneous charge-density wave phase has been suggested by Nabutovskii et al. [28] and discussed by Høye and Stell [29] and Fisher [1]. Evidence for tricritical behavior in restricted primitive lattice models for ionic fluids has

been reported by Dickman and Stell [30] and by Panagiotopoulos and Kumar [31]. In our system at higher salt concentrations, the 3-methylpyridine molecules are assumed to be shielded from the ions by water molecules. In turn, the ions may form a double layer over the water molecules forming a charge layering or microemulsion sponge-like domains.

4. FORMATION OF A THIRD PHASE

Another intriguing phenomenon that we encountered during our investigations of the samples was the observation of a small amount of a third soap-like phase on the interface. We originally observed this phase in the system 3-methylpyridine + water + sodium bromide at approximately 16.5 mass% of NaBr, i.e., very close to the discovered multicritical point. It appeared on the interface immediately after phase separation of the sample. The experiments were performed near the lower consolute temperature. The samples were heated slowly from the one-phase region to the critical temperature. Although the third phase was observed on the interface very close to the critical temperature, the samples were overheated approximately 0.5 K into the two-phase region to observe the third-phase clearly. The samples were filtered with 0.2-μm Millipore filters to ensure that dust was avoided in the samples. These samples were also prepared from chemicals of different purity: NaBr—99.6 and 99.99%; and MP—98, 99, and 99.7%. The third phase was observed independent of any of the above mentioned conditions. The amount of the third phase observed was investigated as a function of the concentration of NaBr. Samples with NaBr concentrations up to 27 mass% have been investigated. It was observed that there is no appreciable increase in the amount of the third phase when the concentration of NaBr is increased beyond 17 mass%. On careful further examination, the third phase was also observed in samples with NaBr concentrations as low as 0.1 mass%, although the amount of the third phase was appreciably lower. If NaCl was used instead of NaBr as the salt, the third phase was observed in these samples as well. We also prepared samples with 3MP and heavy water (D_2O), where the phase separation occurs without salt, and traces of the third phase were seen even in these samples. Under a magnification factor of 10, the third phase has a whitish fibrous appearance. If, after the third phase appears on the interface, the samples are cooled back into the one-phase region and shaken well, very fine fiber-like particles could be seen in the samples. We filtered these samples again and repeated the experiments. It was observed that the third phase forms again in these samples, and there is no appreciable change in the value of T_c or in the position of the interface. The samples were prepared in different kinds of

glass tubes and also in quartz tubes, and the formation of the third phase was observed independent of the kind of tube used.

Visual investigations were also carried out on different liquid mixtures in an attempt to characterize this solid-like phase. Samples of 2,6-lutidine + water were prepared to check whether the third phase is seen in this system, although a strong wetting phenomenon might prevent such an observation. The third phase was not observed in this sample. But, on the addition of approximately 3 mass% NaBr to this binary mixture, the third phase clearly appeared at the interface. For a 10% solution of NaBr, the amount of the third phase seemed to be larger than in the case of a 3% solution. It may be that the amount of the third phase was so small in 2,6-lutidine + water, without any NaBr, that it was not visually noticeable.

The third phase has also been observed in mixtures of isobutyric acid (IBA) + water. These samples were prepared with IBA (99%; Aldrich) and deionized water obtained from an Alpha-Q water purification system. The samples were also filtered through 0.2-μm filters. The phenomenon was checked in both pyrex and quartz cells, and no difference was observed. We also reexamined two samples of isobutyric acid + water and isobutyric acid + heavy water studied by Greer [32] many years ago. These samples had been prepared in pyrex glass tubes, and they had not been filtered. Upon close examination, traces of a third phase were observed in these samples also.

The third phase has not been observed in solutions of 3-methylpentane + nitroethane. Since the refractive indices of these two liquids are very close to each other, critical opalescence is greatly reduced, and it was possible to observe the interface at temperatures very close to T_c. But we did not detect any traces of a soap-like phase at the interface in these solutions. It is not clear yet whether the formation of a soap-like phase at the interface is associated with the formation of a microheterogeneous phase in the bulk as observed in the system $3MP + H_2O + NaBr$ or whether it is related to wetting phenomena.

ACKNOWLEDGMENTS

We are indebted to R. W. Gammon for providing us with the capability of observing phase separation in our liquid mixtures, to S. C. Greer for making her samples of isobutyric acid + water available, and to M. E. Fisher, J. M. H. Levelt Sengers, A. Oleinikova, R. A. Narayanan, G. Stell, and H. Weingärtner for stimulating discussions. The research at the University of Maryland is supported by the National Science Foundation under Grant CHE-9805260. The research at the Indian Institute of Science

was supported by the Department of Science and Technology, Government of India.

REFERENCES

1. M. E. Fisher, *J. Stat. Phys.* **75**:1 (1994).
2. G. Stell, *Phys. Rev. A* **45**:7628 (1992); *J. Stat. Phys.* **78**:197 (1995).
3. H. Weingärtner, M. Kleemeier, S. Wiegand, and W. Schröer, *J. Stat. Phys.* **78**:169 (1995).
4. M. A. Anisimov, A. A. Povodyrev, and J. V. Sengers, *Fluid Phase Equil.* **158–160**:537 (1999); M. A. Anisimov, *J. Phys. Cond. Matt.* **12**:A451 (2000).
5. J. M. H. Levelt Sengers, A. H. Harvey, and S. Wiegand, in *Equations of State for Fluids and Fluid Mixtures*, J. V. Sengers, R. F. Kayser, C. J. Peters, and H. J. White Jr., eds. (Elsevier, Amsterdam, 2000), p. 805.
6. R. G. Rubío and F. Ortega, *J. Phys. Cond. Matt.* **12**:A459 (2000).
7. Y. B. Melnichenko, M. A. Anisimov, A. A. Povodyrev, G. D. Wignall, J. V. Sengers, and W. A. Van Hook, *Phys. Rev. Lett.* **79**:5266 (1997).
8. P. G. de Gennes, *Scaling Concepts in Polymer Physics* (Cornell University Press, Ithaca, NY, 1979).
9. I. D. Lawrie and S. Sarbach, in *Phase Transitions and Critical Phenomena*, C. Domb and J. L. Lebowitz, eds. (Academic Press, New York, 1984), Vol. 9, p. 2.
10. T. Narayanan and K. S. Pitzer, *Phys. Rev. Lett.* **73**:3002 (1994); *J. Chem. Phys.* **102**:8118 (1995).
11. J. Jacob, A. Kumar, M. A. Anisimov, A. A. Povodyrev, and J. V. Sengers, *Phys. Rev. E* **58**:2188 (1998).
12. G. M. Schneider, *Ber. Bunsenges. Phys. Chem.* **76**:325 (1972).
13. B. V. Prafulla, T. Narayanan, and A. Kumar, *Phys. Rev. A* **45**:1266 (1992).
14. A. J. Bray and R. F. Chang, *Phys. Rev. A* **12**:2594 (1975).
15. M. E. Fisher and R. J. Burford, *Phys. Rev.* **156**:583 (1967).
16. M. E. Fisher, *Phys. Rev.* **176**:237 (1968).
17. M. A. Anisimov, E. E. Gorodetskii, V. D. Kulikov, and J. V. Sengers, *Phys. Rev. E* **51**:1199 (1995).
18. H. Y. Cheng, M. A. Anisimov, and J. V. Sengers, *Fluid Phase Equil.* **128**:67 (1997).
19. M. A. Anisimov, A. A. Povodyrev, V. D. Kulikov, and J. V. Sengers, *Phys. Rev. Lett.* **75**:3146 (1995).
20. M. A. Anisimov, A. S. Kurlandsky, and N. F. Kazakova, *Mol. Cryst. Liq. Cryst.* **159**:87 (1988).
21. J. Jacob, A. Kumar, S. Asokan, D. Sen, R. Chitra, and S. Mazumder, *Chem. Phys. Lett.* **304**:180 (1999).
22. M. Misawa, K. Yoshida, K. Maruyama, H. Munemura, and Y. Hosokawa, *J. Phys. Chem. Solids* **60**:1301 (1999).
23. E. Luijten and K. Binder, *Phys. Rev. E* **58**:R4060 (1988).
24. M. A. Anisimov, E. Luijten, V. A. Agayan, J. V. Sengers, and K. Binder, *Phys. Lett. A* **264**:63 (1999).
25. A. A. Povodyrev, M. A. Anisimov, and J. V. Sengers, *Physica A* **264**:345 (1999).
26. C. M. Knobler and R. L. Scott, in *Phase Transitions and Critical Phenomena*, C. Domb and J. L. Lebowitz, eds. (Academic Press, New York, 1984), Vol. 9, p. 164.
27. L. D. Landau and E. M. Lifshitz, *Statisticheskaya Fizika*, Part 1, 5th Russian ed. (Fizmatlit, Moscow, 1995).

28. V. M. Nabutovskii, N. A. Nemov, and Yu. G. Peisakhovich, *Zh. Eksp. Teor. Fiz.* **79**:2196 (1980) [*Sov. Phys. JETP* **52**:1111 (1980)]; *Phys. Lett. A* **79**:98 (1980); *Mol. Phys.* **54**:979 (1985).
29. J. S. Høye and G. Stell, *J. Phys. Chem.* **94**:7899 (1990).
30. R. Dickman and G. Stell, in *Simulation and Theory of Electrostatic Interactions in Solution*, L. R. Pratt and G. Hummer, eds. (American Institute of Physics, New York, 1999), p. 225; G. Stell, in *New Approaches to Problems in Liquid State Theory*, C. Caccamo, J. P. Hansen, and G. Stell, eds. (Kluwer, Dordrecht, 1999), p. 71.
31. A. Z. Panagiotopoulos and S. K. Kumar, *Phys. Rev. Lett.* **83**:2981 (1999).
32. S. C. Greer, *Phys. Rev. A* **14**:1770 (1976); *Ber. Bunsenges. Physik. Chem.* **81**:1079 (1977).